CONDUCTIVITY OF METALLIC SURFACES AT MICROWAVE FREQUENCIES

E. MAXWELL

TECHNICAL REPORT NO. 21

Conductivity of Metallic Surfaces at Microwave Frequencies*

E. MAXWELL

Research Laboratory of Electronics, Massachusetts Institute of Technology, Cambridge, Massachusetts

(Received February 4, 1947)

Methods of measuring effective conductivities at microwave frequencies are described. These consist of either measuring the transmission loss in a long waveguide, or in measuring the Q's of resonant cavities. Both methods have been applied to measurements at 1.25 cm. Results for a number of metals are presented. Deviations from d.c. conductivity are thought to be due to surface roughness.

1. INTRODUCTION

IN the course of development of microwave components it was early observed that the high frequency conductivity of many metallic surfaces was frequently lower than the d.c. conductivity. This phenomenon was especially noticeable in the 1.25-cm region. The work described here was done for the purpose of collecting data on the conductivities of representative surfaces in the region of 1.25 cm.

The r-f conductivity is important in at least two applications. These are:

(1) Long transmission systems where the total attenuation is governed by the conductivity.

(2) Cavity resonators, in which the maximum attainable Q is limited by the effective conductivity.

The effective conductivity of metals at microwave frequencies is governed by a superficially thin surface layer. The current density inside the metal decreases exponentially with depth according to $J = J_0 \exp{-[(\omega\mu\sigma/2)]^{\frac{1}{2}}x}$, where $J_0 =$ current density at the surface, $\omega =$ angular frequency, $\mu =$ permeability, $\sigma =$ conductivity, and $x =$ distance into conductor measured along the normal.

When $x = (2/\omega\mu\sigma)^{\frac{1}{2}}$, $J = J_0/e$. This value of x is defined as the skin depth δ. It is easy to show that the total loss, obtained by integrating $J^2/2\sigma$ with respect to x, (between 0 and ∞), is equal to $J_0^2/2\sigma\delta$. For purposes of calculating losses one may consider the current confined to a skin of thickness δ within which the current density is

uniform and equal to J_0. Actually of course 37 percent of the total current flows at depths below δ.

This formulation is rigorously correct only for an infinite plane surface. However, it remains an excellent approximation for curved surfaces whose radii of curvature are large compared to δ. In computing losses one evaluates the integral

$$\iint\limits_{S} \frac{J_0^2}{2\sigma}ds = \iint\limits_{S} \frac{H_t^2}{2\sigma}ds$$

taken over the surface of the waveguide or cavity. H_t is the tangential component of magnetic field. (The factor 2 comes in since we are interested in average power dissipation, and J_0. and H_t are both maximum values of sinusoidal time functions.) If the metal surface is not smooth but has surface irregularities and scratches whose dimensions are comparable with δ, the foregoing treatment is evidently an over-simplification. The presence of scratches may alter the current distribution especially if the scratches are in a direction orthogonal to the lines of current flow. The scratches could conceivably act like constrictions in the effective cross section, thereby increasing the resistance.

2. MEASURING TECHNIQUES

Two general methods of measurement have been employed. In the first method the sample to be measured is in the form of a long piece of waveguide or equivalent transmission system. If one end of the waveguide is shorted, the standing-wave ratio seen looking into the other end is a known function of the guide attenuation, which in turn depends on the conductivity. Thus, from a single measurement of standing-wave
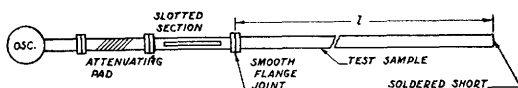
Fig. 1. Attenuation measurement by long guide technique. Rectangular guide.

ratio, the effective conductivity may be computed.

In the second method, the sample forms the walls of a resonant cavity. The Q of the cavity is a known function of the conductivity, and hence the conductivity may be calculated from the measured Q. A variation of this method was found quite useful. The input conductance at resonance is directly proportional to the losses in the cavity, or more precisely, to the square root of the wall resistivity. The constant of proportionality depends on the coupling and, if known, a single measurement of the input standing-wave ratio at resonance permits one to calculate the resistivity.

2.1 DETAILS OF FIRST METHOD

The measurement set-up for rectangular wave guide is illustrated in Fig. 1. If r is the measured voltage standing-wave ratio, and l is the length of the wave guide, the attenuation is given as follows:

Attenuation per unit length $= \alpha$

$$= -\frac{10}{l} \log_{10}\left(\frac{r-1}{r+1}\right) \text{ db}$$

$$= -\frac{1}{2l} \log_e\left(\frac{r-1}{r+1}\right) \text{ nepers.}$$

The attenuation and conductivity are related by the following expression:

$$\alpha = \frac{1}{2b} \cdot \frac{1}{[1-(\lambda_0/\lambda_c)^2]^{\frac{1}{2}}} \cdot \left(\frac{4\pi}{\lambda_0\mu c\sigma}\right)^{\frac{1}{2}} \cdot \left[1+\frac{2b}{a}\left(\frac{\lambda_0}{\lambda_c}\right)^2\right],$$

where $\alpha =$ attenuation in nepers per meter, $\sigma =$ conductivity in mhos per meter, $a =$ wave guide width in meters, $b =$ waveguide height in meters, $\lambda_0 =$ free space wave-length in meters, $\lambda_c = 2a =$ guide cut-off wave-length in meters, $\mu_0 =$ permeability of free space (M.K.S.) $= 4\pi \times 10^{-7}$, and $c =$ velocity of light $= 3 \times 10^8$ meters per second. This expression is for the TE_{10} mode

only. For $0.170'' \times 0.420''$ wave guide at 1.25 cm, the formula reduces to:

$$\alpha = 299/(\sigma)^{\frac{1}{2}} \text{ nepers per meter.}$$

The length of waveguide is conveniently chosen so as to have a voltage standing-wave ratio of about 5 or 6. At 1.25 cm with common materials, this usually means a waveguide length of the order of six feet. The correction for losses in the slotted section is then negligible.

The far end of the waveguide should be shorted by means of a soldered plate. A choke plunger is unsatisfactory for this purpose, since some power may leak past. If the waveguide is suspected of inhomogeneities or bad spots, a quarter wave-length should be removed from the shorted end and the test repeated. This will shift the standing-wave pattern by a quarter wave-length, and if bad spots are present, the measured loss will probably be different in the two cases. The loss in the short circuiting plate is of course negligible in comparison to that in the wave guide itself.

The foregoing procedure is straightforward enough when dealing with rectangular wave guide. Frequently, however, one wishes to use circular waveguide. This can be done by using a round-to-rectangular transition piece, or transformer, between the round pipe and the slotted section, but a special technique must be employed to avoid errors due to elliptical polarization in the pipe.

It is inevitable that any long piece of round pipe will have both ellipticity and skewness which will cause the incident wave to split up into a pair of cross-polarized waves. Each of these cross-polarized waves will be reflected at the short and come back down the pipe, but only the vertical component of each will couple into the rectangular waveguide. This will cause the observed standing-wave ratio in the rectangular slotted section to be less than the true standing-wave ratio at the sending end of the round pipe.

This difficulty may be eliminated as follows. It may be shown theoretically that given any skewed elliptical pipe, it is possible to choose a direction of polarization for the incident wave, such that the reflected wave arrives with that same polarization. The reflected wave then couples completely into the rectangular wave

630

guide. and the standing-wave ratio observed in the slotted section is the true standing-wave ratio.

If the pipe is a perfect elliptic cylinder, it is clear that either of the principal axes of the ellipse may be taken as the preferred direction. An actual pipe is more apt to resemble a twisted cylinder in which both the orientation of the axes and the ellipticity are functions of position along the axis of propagation. Thus there may be cross-coupling between the modes, and the reflected wave will not generally have the same orientation as the incident wave.

In practice the round wave guide is arranged so that it may be rotated with respect to the transformer (see Fig. 2). The wave guide is rotated until the position of the maximum standing-wave ratio is found. This is the condition for which the reflected wave returns with the same polarization as the incident wave. A convenient type of round-to-rectangular transformer is a quarter wave-length of oval cross section intermediate in shape between the round and rectangular sections. The loss in such a transformer is quite negligible.

This technique was applied in measuring the effective conductivity of mercury. A circular waveguide was constructed by immersing a polystyrene rod in mercury. The details of this experiment are described in the Appendix.

2.2 DETAILS OF SECOND METHOD

In any resonant cavity, the unloaded Q is given by

$$Q_0 = \text{const.} \times \frac{\lambda}{\delta},$$

where λ is the resonant wave-length, and δ is the skin depth. The constant of proportionality is a function of the resonator geometry and is known for many of the simpler cases. Thus if one measures Q_0, it is simple to compute the effective conductivity from δ (if the resonator geometry is one for which the theoretical problem has been solved).

In practice, one couples a waveguide into the cavity by means of a coupling window of some sort and measures the variation of input standing-wave ratio with frequency. The half width
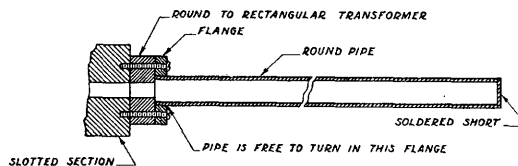

FIG. 2. Attenuation measurement by long guide technique. Round guide.

of the resulting resonance curve determines Q_L, the loaded Q. Thus,

$$\frac{1}{2Q_L} = \frac{\omega_i - \omega_0}{\omega_0} \tag{1}$$

where ω_0 is the resonant frequency and ω_i the frequency corresponding to the half-power point. (The half-power point is the frequency at which the power absorbed by the cavity is half the power absorbed at resonance.) The ordinates of the half-power points are given by

$$\beta_i = \frac{\beta_0 + 1 + (\beta_0{}^2 + 1)^{\frac{1}{2}}}{\beta_0 + 1 - (\beta_0{}^2 + 1)^{\frac{1}{2}}}, \tag{2}$$

where $\beta_0 = $ the voltage standing wave ratio at resonance, and $\beta_i = $ the voltage standing wave ratio at the half-power point.

The loaded and unloaded Q's are related by

$$\frac{Q_0}{Q_L} = 1 + \frac{Y_0}{G}, \tag{3}$$

where $Y_0 = $ the line admittance, and $G = $ the input conductance of the cavity. If the cavity is under-coupled,

$$Y_0/G = 1/\beta_0 \tag{4a}$$

and if overcoupled

$$Y_0/G = \beta_0. \tag{4b}$$

The existence of undercoupling or overcoupling is determined experimentally by the presence of a minimum or a maximum, respectively, at the input window.

A calculating technique which makes somewhat better use of the data is as follows: The equation of the resonance curve is:

$$\left(\frac{2\Delta Q_0 G}{Y_0}\right)^2 \frac{Y_0}{G} + \frac{Y_0}{G} + \frac{G}{Y_0} = \frac{1 + \beta^2}{\beta}, \tag{5}$$
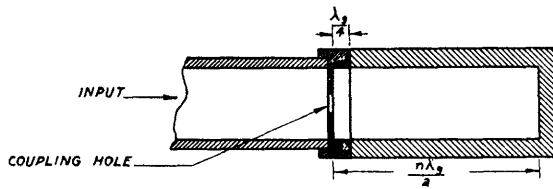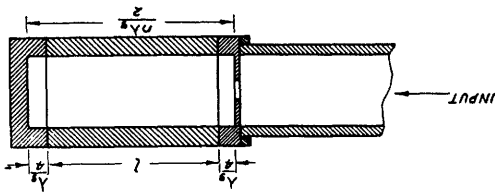
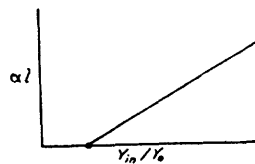FIG. 3a. Two part resonator.

FIG. 3b. Three part resonator.

FIG. 3c. Calibration plot.

where $\Delta = (\omega - \omega_0/\omega_0)$, and β = voltage standing wave ratio at frequency ω. If one plots $(1 + \beta^2/\beta)$ vs. Δ^2, a straight line is obtained. By fitting the best straight line to the experimental data, one may evaluate Q_0, Q_L, and Y_0/G. This procedure makes use of the entire resonance curve and not merely three points.

It is thus clear that one may determine Q_0 from bandwidth measurements and, having found it, calculate the corresponding effective conductivity of the wall material. In principle then, one may construct a series of cavities from the various materials to be tested and evaluate the effective conductivities by the methods described above.

Although this technique is straightforward, there were a number of practical reasons which militated against its use in this investigation. First of all, the active surfaces, being the interior walls of the cavity, would not always be readily accessible for polishing, plating, or other surface treatment. Secondly, the bandwidth measurements were tedious and difficult with the techniques then available, and since many measurements were to be made, they would have proved very time consuming. The bandwidth measurements require stable oscillators and means for measuring accurately small frequency intervals. Although such equipment is available today, it was not at the time this work was begun. Therefore, a modified technique was developed in which a minimum of bandwidth measurements was required.

Suppose we consider a cavity which is feeding power back to the line, instead of absorbing power from the line. This would be the case when the oscillator is shut off, and the field in the cavity starts to decay. Then,

$$Q_0 = 2\pi \frac{\text{Energy stored in the cavity}}{\text{Energy dissipated in cavity walls per cycle}}, \tag{6a}$$

$$Q_L = 2\pi \frac{\text{Energy stored in the cavity}}{\text{Energy dissipated in cavity walls} + \text{energy radiated back to line per cycle}}, \tag{6b}$$

$$Q_W = 2\pi \frac{\text{Energy stored in the cavity}}{\text{Energy radiated back to line per cycle}}. \tag{6c}$$

Q_W is the window Q, or external Q. It depends only on the shape of the cavity and the geometry of the coupling window and not upon the conductivity of the walls.

Evidently,

$$1/Q_L = (1/Q_0) + (1/Q_W). \tag{7}$$

Also since

$$Q_0/Q_L = 1 + (Y_0/G), \quad Y_0/G = Q_0/Q_W. \tag{8}$$

Equation (8) means that the standing-wave ratio at resonance, or its reciprocal, is proportional to the unloaded Q.

632

Thus in principle, if we have a series of cavities which are identical in all dimensions, including those of the coupling window, the input standing-wave ratio of each cavity will be proportional to its Q, and the constant of proportionality is the same for all cavities. A bandwidth measurement on just one of the cavities will suffice to determine the window Q, and thus the constant of proportionality. The fact is, however, that the window Q varies very rapidly with the coupling window dimensions, so that it is impracticable to maintain the necessary tolerances.

A more practical approach is to build a cavity in two or more demountable sections, such that the test piece may form one of these sections. Examples of this type of construction are indicated in Figs. 3–6.

The first one tried was the TE_{011} resonator of Fig. 5a. The removable sample is the end plate. The lines of current flow are coaxial circles and nowhere cross the contact surface, so that the losses in the oscillating mode are not affected by the contact resistance. There is considerable advantage in having the sample in the form of a flat plate, since this is the most convenient form for cleaning, polishing, plating, etc. This resonator had two serious disadvantages, however. First of all, the TE_{011} mode is intrinsically degenerate with the TM_{111} odd and even modes, so that extreme care must be taken to avoid exciting these modes (if it can be avoided at all).
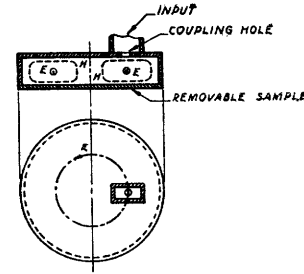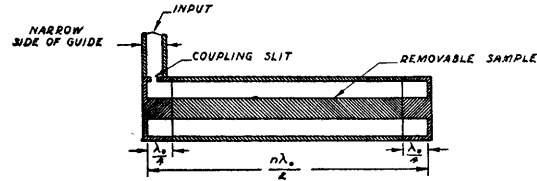

FIG. 5a. TE_{011} mode resonator.
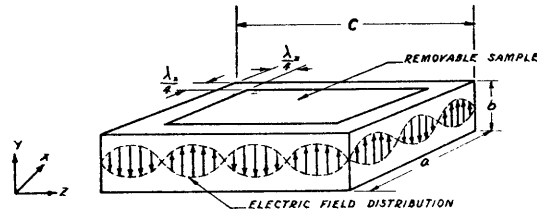

FIG. 5b. Coaxial resonator—TEM mode.

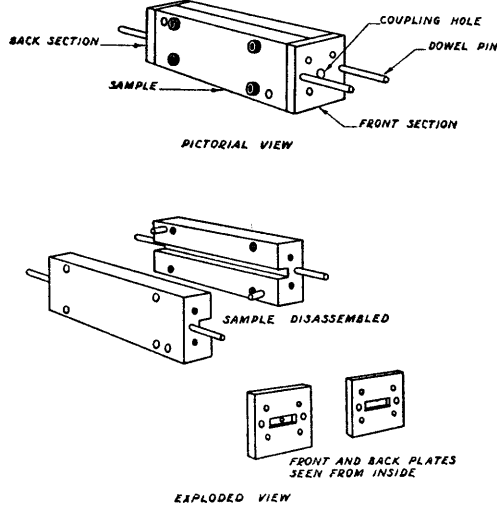FIG. 6. Rectangular resonator.

Secondly, there are a number of non-resonant modes present in the cavity which influence the window Q in an undesirable fashion. This trouble seems to arise whenever we use a resonator whose dimensions are such that more than one mode can propagate in the cavity, even though the unwanted modes are non-resonant. For the cavity shown in Fig. 5a, the TE_{11}, TM_{01}, and TE_{21} modes, which are lower than the TE_{01}, will certainly propagate along the axis of the cylinder, and in addition many higher ones will also propagate because of the relatively large diameter. (A squat cavity was chosen in order to make the ratio of sample loss to total loss as large as possible.) These extraneous modes are excited because the presence of the coupling hole, or slit, imposes boundary conditions which cannot be satisfied by the resonant mode alone. The currents which flow, as a result of these modes, do cross the contact surfaces and are therefore controlled by the contact resistance.

FIG. 4. Rectangular resonator details.

The energy stored in these modes determines the equivalent susceptance of the coupling iris and hence the window Q. In other words, the window Q depends upon the contact resistance which is not a reproducible quantity. Therefore, the window Q varies from measurement to measurement and must be redetermined each time. Since it was desired to eliminate bandwidth measurements, this type of resonator was discarded.

There is, however, considerable merit in using flat plate samples. With the stabilized oscillators now available,[1] bandwidth measurements in the region of 24,000 Mc are no longer difficult so that the method of the preceding paragraph is entirely practicable today. The TE_{011} cavity is not the best choice, however, owing to the degeneracy with the TM_{111} modes. A suggested cavity, using a removable flat plate sample, is illustrated in Fig. 6. This would operate in the TE_{l0n} mode. By choosing the dimensions such that $b < \lambda_0/2$, and if a and b are incommensurable, one may avoid accidental degeneracies. The resonant wave-length λ_0 is determined from the relation $(2/\lambda_0)^2 = (l/a)^2 + (n/c)^2$ in which l and n are equal to the number of half-period variations along the x and z axes, respectively. The contact surfaces are at current nodes. A cylindrical cavity in the TM_{0m0} mode could be used as well, in which case the sample plate would be circular.

Figure 5b illustrates another type of demountable cavity in which the sample is the removable center conductor. This resonator operates in the principal mode. The breaks in the inner and outer conductors occur at points of zero current. One version of this was tried in which the diameter was large enough so that the TE_{11} mode could propagate. Here again it was found that the window Q was not reproducible.

The cavity finally chosen for making most of the measurements was the demountable rectangular type illustrated in Figs. 3 and 4. This was taken as the best compromise between the conflicting requirements of convenient sample shape and simplicity of measuring technique. The cavity operates in the lowest mode, the

[1] R. V. Pound, Radiation Laboratory Report 662; R. V. Pound, Radiation Laboratory Report 837; and R. V. Pound, "Electronic Frequency Stabilization of Microwave Oscillators," Rev. Sci. Inst. 17, 490 (1946).

TE_{10n}. The cross-sectional dimensions are standard waveguide dimensions for 1.25 cm, and therefore modes higher than the TE_{10} cannot propagate. The higher modes generated in the vicinity of the coupling window are damped out very rapidly. The breaks in the walls occur across lines of no current flow and are sufficiently removed from the neighborhood of the coupling window so that the higher mode amplitude is practically nil.

Both two- and three-section cavities were used, although the three-section type is preferred because it is easier to get at the active surfaces. An exploded view of the three-part resonator is shown in Fig. 4.

The normalized input conductance at resonance is:

$$G/Y_0 = Q_w/Q_0. \tag{8a}$$

For the simple rectangular resonators used this may be written in the form

$$\frac{G}{Y_0} = \frac{n\pi B^2}{2Q_0}\left(\frac{\lambda_g}{\lambda_0}\right)^2 = \left(\frac{B}{Y_0}\right)^2 (\alpha l + R), \tag{9}$$

where $n =$ the axial length in numbers of half wave-lengths, $\lambda_g =$ the guide wave-length, $\lambda_0 =$ the free space wave-length, $B =$ the susceptance of the coupling window, $\alpha =$ the attenuation in the sample portion in nepers/meter, $l =$ the length of the sample portion, and $R =$ a resistance which represents the dissipation in the front and back quarter-wave sections.

In the above formula (αl) is the total attenuation in the sample. The relation between (αl) and G/Y_0 is linear. A convenient way to calibrate a pair of front and back quarter-wave sections is as follows. The attenuation in a long piece of waveguide is measured by the short-circuited guide technique described earlier in this paper. Samples with different values of (αl) are obtained by cutting this piece up into short sections, each one of which is a different multiple of a half wave-length. From the data taken with these samples a calibration plot of total attenuation in the sample vs. input conductance is obtained as in Fig. 3c.

This calibration plot is then used to determine the attenuation in unknown samples. The sample

TABLE I. Conductor losses in standard K-band waveguide.[1]

Material	Measured atten. in db/meter	Calculated[2] atten. in db/meter	Meas. atten. / Calc. atten.	Eff. cond. at K-band in 10^7 mho/m	d.-c. Cond. in 10^7 mho/m
Aluminum[7]					
Pure, commercial (machined surface)	0.58	0.455	1.27	1.97	3.25 (measured)
17S Alloy[7] (machined surface)	0.75	0.586	1.28	1.19	1.95 (measured)
24S Alloy (machined-surface)	0.66	0.635	1.04	1.54	1.66 (measured)
Brass					
Yellow (80-20) drawn wave guide	0.68	0.653	1.04	1.45	1.57 (measured)
Red (85-15) drawn wave guide	0.55			2.22	
Yellow round drawn tubing[3]	0.90	0.844	1.07	1.36	1.56 (measured)
Yellow (80-20) (machined surface)	0.76	0.653	1.15	1.17	1.57 (measured)
Free machining brass (mach. surface)	0.75	0.673	1.12	1.11	1.48 (measured)
Cadmium plate	0.79-0.87	0.711	1.13-1.22	1.04-0.89	1.33 Hdbk. of Phys. and Chem.
Chromium plate, dull[4]	0.67-0.82	0.418	1.60-1.96	1.49-0.99	3.84 Hdbk. of Phys. and Chem.
Copper					
Drawn O.F.C. wave guide	0.41	0.350	1.17	4.00	5.48 (measured)
Drawn round tubing	0.52	0.496	1.05	4.10	4.50 (measured)
Machined surface[7]	0.38	0.349	1.09	4.65	5.50 (measured)
Copper plate	0.54-0.61	0.337	1.60-1.81	2.28-1.81	5.92 }Hdbk. of Phys. and Chem.
Electroformed wave guide[7]	0.46	0.337	1.37	3.15	5.92
Gold plate	0.60	0.404	1.48	1.87	4.10 Hdbk. of Phys. and Chem.
Iron, electroformed[7]	1.01				
Mercury[6]	2.50	2.54	0.98	0.104	0.104 Hdbk. of Phys. and Chem.
Monel (machined surface)[5,7]	2.08	2.07	1.01	0.155	0.156 (measured)
Nickel[7]					
Electroformed wave guide	0.82				
Nickel plate	1.11				
Silver					
Coin silver drawn wave guide	0.45	0.375	1.20	3.33	4.79 (measured)
Coin silver lined wave guide	0.60	0.375	1.60	1.87	4.79 (assumed)
Coin silver (machined surface)[7]	0.51	0.375	1.34	2.66	
Fine silver (machined surface)[7]	0.48	0.330	1.45	2.92	6.14 Hdbk. of Phys. and Chem.
Silver plate	0.41-0.57	0.330	1.24-1.73	3.98-2.05	
Solder, soft[7]	1.05	0.978	1.08	.600	0.70 (measured)
Steel, cold rolled (mach. surface)	2.85				

[1] Unless otherwise noted, figures are for TE_{10} mode, $\lambda = 1.25$ cm in rectangular guide of dimensions of 0.170″ X0.420″.
[2] Theoretical attenuation for TE_{10} mode in 0.170″ X0.420″ rectangular waveguide at 1.25 cm is $2590\sigma^{-\frac{1}{2}}$ db/m where σ is given in mho/meters. For the TE_{11} mode in round pipe at 1.25 cm, the attenuation is $3330\sigma^{-\frac{1}{2}}$ db/m.
[3] 0.345″ I.D., TE_{11} mode.
[4] No nickel undercoat.
[5] This surface was somewhat rougher than most machined surfaces.
[6] For method of measurement refer to the Appendix. Figures are expressed for a guide of 0.170″ X0.420″ cross section.
[7] Only one sample of these was tested.

may be any multiple of a half wave-length. However, for any given window susceptance there is a range of sample attenuations which produce conveniently measurable standing-wave ratios. It is a good idea to plate the front and back sections with some corrosion-resistant material to insure permanence of calibration.

3. EXPERIMENTAL RESULTS

The more important available data on conductor losses at 1.25 cm are summarized in Table I. These are expressed in terms of attenuation of the TE_{10} mode in standard 0.170″ X0.420″ waveguide at 1.25 cm, or in some cases for the TE_{11} mode in round pipe of 0.345″ diameter. The first column records the value of the experimentally measured attenuation, the second that of the theoretically computed attenuation, and the third column gives the ratio of the two; the fourth and fifth columns list the effective conductivity at 1.25 cm and the d.c. conductivity, respectively.

The theoretical attenuations are computed by means of the formulas given in the footnotes of Table I. The conductivities used in these formulas are the d.c. conductivities listed in the fifth column. The d.c. conductivity of the samples was measured wherever possible but in some cases it was not convenient or possible to do so. In these other cases, the sources from which the d.c. conductivity data were taken, are indicated. In comparing theoretical and experimental performance it is important to have accurate data on the d.c. conductivities if the comparison is to have much significance. In the case of fairly pure materials, such as mercury or electrodeposited metals, the conductivity figures given in handbooks for pure metals are probably good enough, but for commercial metals and alloys there may be discrepancies between tabulated and actual values.

Although the listing is far from complete, many of the common conductor materials are present. There is usually some variation in con-

ductivity among different specimens of the same material, particularly in machined and electroplated surfaces. Where the variation among specimens was more than a few percent, the outside limits of attenuation are stated in the table. Some of the figures are based on a single specimen and are so indicated. In the other cases anywhere from two to about six samples were tested. The probable error to be associated with the attenuation figures is estimated as less than two percent. In the case of the soft solder the error may be of the order of 10 percent since the measurement quoted here is of an earlier vintage than the others and the technique employed was less accurate.

The surfaces examined fall into three categories: drawn, machined, and electrodeposited. The drawn surfaces are as a rule quite good and although their losses are greater than theory predicts, the discrepancy is not large. In the case of brass it may amount to only 5 percent. Machined surfaces are frequently poorer, while plated surfaces seem to vary a good deal.

It seems reasonable to assume that the increase in r-f conductivity over the d.c. value is due primarily to surface roughness. It is difficult, however, to establish such a correlation on the basis of the observed data since no reliable index of surface roughness is available for the samples tested.

The measurement of the r-f conductivity of mercury, which was briefly mentioned earlier, is of interest in this connection. In this experiment the attenuation was measured in a waveguide made by immersing a smooth polystyrene rod in mercury. Because of the surface tension of the mercury, the resulting surface was considered to be free from the usual multitude of scratches and crevices present on solid metallic surfaces.

Table II. Conductor losses in K-band waveguide with protective coatings.

Material	Measured attenuation in db/meter
Palladium flash (10^{-5} in.) on coin silver	0.6
Rhodium flash (10^{-5} in.) on coin silver	1.0
Sperry f710 lacquer on copper plate	1.2
Same surface without lacquer	0.6
Zinc chromate olive drab primer on 17S aluminum alloy	1.0

Furthermore, since the skin depth is about eight times as big in mercury as in copper or silver, such irregularities as remain are relatively less important. The measured attenuation agreed with the calculated value within 2 percent which was about as accurately as the standing-wave ratio could be measured. Actually, however, the experimental figure may be in doubt by 4 or 5 percent as a result of a possible uncertainty in the assumed value of the conductivity of coin silver which enters into the experiment. The fact that agreement was attained here between theory and experiment again implies that the lack of agreement observed in other cases is due to surface irregularity. This matter is discussed in the Appendix where the experiment is described in detail.

It should be noted that for the monel sample also, there is substantial agreement between observed and calculated attenuations. The skin depth in monel is approximately the same as in mercury. Thus one may infer that because of the greater skin depth the scratches are less important.

Many attempts were made to improve the conductivity of samples by polishing the active surfaces by both mechanical and electrolytic methods, but none of these were successful. Probably something of the order of a metallographic or optical polish is necessary, but it was not possible to approach this degree of excellency on account of the awkward shape of the surfaces to be polished. In this connection, flat samples would be decidedly advantageous.

The reverse process was possible. The conductivity was definitely lowered in many cases by abrading the surface. For example, when some yellow brass waveguide tubing was broached out, the attenuation was increased from 0.68 db/m to 0.74 db/m.

Thin oxide films are not harmful as long as the oxide resistivity is high. It may be shown that the effect of oxide films is small as long as the skin depth in the oxide material is large compared to the oxide layer thickness.

The effect of a few protective coatings in increasing attenuation is shown in Table II.

Of all the solid metals listed mild steel has the greatest loss. This behavior has been explained

636

by Kittel on the basis of the magnetic proper-
ties.[2]

ACKNOWLEDGMENT

I am indebted to Dr. E. M. Purcell, formerly
of the Radiation Laboratory, for many helpful
suggestions.

APPENDIX

The Mercury Waveguide Experiment

The experimental setup is indicated in Figs.
7a and 7b. The wave guide consisted of a round
polystyrene rod immersed in mercury. This was
tapered into a round air-filled guide as shown
in Fig. 7b. A round-to-rectangular transition
coupled the round guide to a standard rectan-
gular slotted section. The rod was then treated
as a shorted round waveguide and the attenu-
ation measured by the techniques described
under method I for round guide.

The dielectric losses were separated from the
conductor losses in the following manner. Before
setting up the mercury guide a tightly fitting
drawn coin silver tube was slipped over the
polystyrene rod, as in Fig. 7a. The input
standing-wave ratio was measured, and from
this the total attenuation in the polystyrene-
silver guide was calculated. The silver tube was
then removed and the polystyrene rod immersed
in mercury as in Fig. 7b. The standing-wave
ratio was again measured and the attenuation
in the polystyrene system calculated. The dif-
ference between these two figures is the con-
ductor attenuation in the mercury minus the
conductor attenuation in the coin silver. The
attenuation in the coin silver was calculated by
using the effective conductivity established from
previous measurements on drawn rectangular
coin silver wave guide, and the attenuation due
to the mercury was determined. The attenuation
thus found agreed with theory within 2 percent.

An estimate of the limit of error was made on
the following basis. The attenuation in the
polystyrene-silver system was 1.46 db; in the
polystyrene-mercury system it was 3.29 db,
mercury attenuation less silver attenuation

[2] C. Kittel, "Theory of the dispersion of magnetic
permeability in ferromagnetic materials at microwave
frequencies," Phys. Rev. 70, 281 (1946).
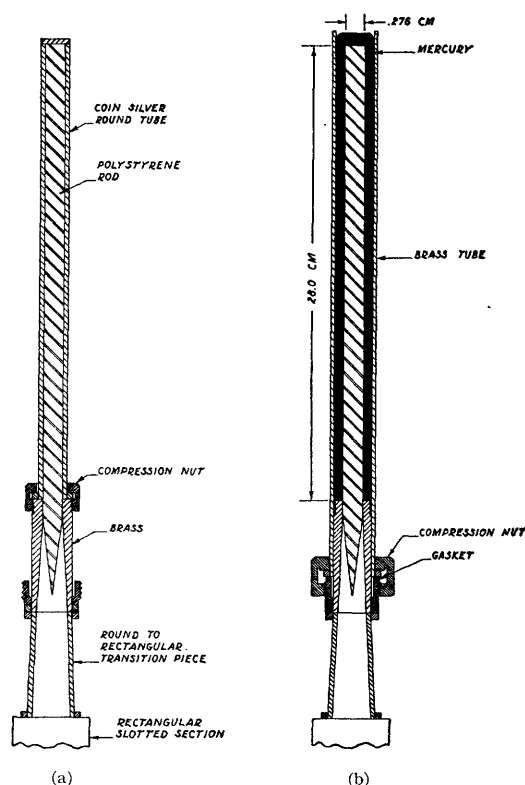
FIGS. 7a and 7b. Mercury wave guide.

= 1.83 db. The effective conductivity of coin
silver wave guide is 3.3×10^7 mhos per meter.
The conductor attenuation for the TE_{11} mode
in the silver tube was 0.40 db for a 28 cm length
(see Fig. 7b). The net loss due to the mercury
alone was therefore 2.23 db or 8.0 db per meter.
The value calculated by using the tabulated
figure of 0.1044×10^7 mhos per meter for mercury
at 20°C, was 8.10 db per meter. The error depends
largely on the accuracy of the assumed attenua-
tion for the coin silver. By assuming a 20 percent
error in estimating the attenuation in silver,
which should certainly be an outside figure, the
uncertainty in the mercury attenuation would be
less than 4 percent.

It should also be pointed out that residual
mismatch in the taper or transition causes very
little error because of the fact that the mismatch
appears in both measurements and almost com-
pletely cancels out in the final result. As a pre-
liminary part of the experiment, taper and
transition mismatch was investigated by slipping

some close fitting poly-iron sleeves over the polystyrene rod, in place of the silver tube, so as to obtain a matched absorbing load. The voltage standing-wave ratio looking in was 1.08. It may be verified by calculation that in the worst case this would make an error of less than $\frac{1}{2}$ percent.

Formula Used in Computing Attenuation:[3]

---

[3] See J. A. Stratton, *Electromagnetic Theory* (McGraw-Hill Book Company, Inc., 1941), p. 544.

$$\alpha = \frac{1}{a}\left(\frac{\pi\epsilon\nu}{\sigma}\right)^{\frac{1}{2}}\left[1-\left(\frac{\nu_{11}'}{\nu}\right)^2\right]^{-\frac{1}{2}}$$

$$\times\left[\left(\frac{\nu_{11}'}{\nu}\right)^2 + \frac{1/u_{11}'^2}{1-1/u_{11}'^2}\right].$$

a = radius of polystyrene rod, $\epsilon = 2.52\epsilon_0$ for polystyrene, $u_{11}' = 1.84$, $\nu_{11}' = [u_{11}'/2\pi a(\epsilon\mu)^{\frac{1}{2}}]$, and ν = frequency. M.K.S. units used.